

Phase Separation in Polystyrene–Poly(vinyl methyl ether) Blends Dilated with Compressed Carbon Dioxide

Vijayakumar S. RamachandraRao and James J. Watkins*

Department of Chemical Engineering, University of Massachusetts, Amherst, Massachusetts 01003

Received January 18, 2000; Revised Manuscript Received April 24, 2000

ABSTRACT: The phase behavior of polystyrene (PS)/poly(vinyl methyl ether) (PVME) blends of various compositions in the presence of compressed carbon dioxide was investigated using in-situ high-pressure fluorescence spectroscopy. Sorption of a few weight percent of CO₂, which is a poor solvent for both components but selective for PVME, induces phase separation at 40 and 60 °C for all compositions studied. These transitions occur as much as 90 °C below the coexistence temperatures for the corresponding binary blends at ambient pressure. The Sanchez–Lacombe equation of state qualitatively predicts phase separation in the PS/PVME/CO₂ system as CO₂ pressure is increased isothermally. A semiquantitative stability analysis suggests that a disparity in the free volumes of the polymer components upon dilation with carbon dioxide, rather than enthalpic contributions, is the principal driver for phase separation in this system.

Introduction

The effect of solvent on polymer compatibility in mixtures and block copolymers has important consequences for materials processing. Numerous theoretical and experimental studies have demonstrated that the addition of liquid solvents can either suppress or induce polymer phase separation in blends depending on the relative quality of the solvent for each of the constituents.^{1–4} Recently, these concepts have been applied to shifting the location of order–disorder transitions (ODTs) in block copolymers.^{5–7} To date, virtually all studies have focused on liquid solvents. We have initiated a program to examine the influence of compressible fluid sorption on polymer compatibility in blends and diblock copolymer systems near both upper and lower critical solution transitions.^{8,9} This work is motivated by two factors: First, an understanding of the phase behavior of multicomponent polymer systems in the presence of compressible fluids is a prerequisite for the continued development of supercritical fluid processing options. Second, the consequences of compressed fluid sorption are thermodynamically distinct from those of liquid solvents (vide infra) and thus may render distinct contributions to compatibility (or segregation).

In our first report, a brief small-angle neutron scattering (SANS) study, we demonstrated that the sorption of low weight fractions of compressed carbon dioxide into symmetric, deuterated polystyrene (d-PS)/poly(vinyl methyl ether) (PVME) blends induced phase segregation at temperatures as much as 115 °C below the ambient pressure transition.⁸ The extreme sensitivity of phase behavior near the lower critical solution temperature (LCST) to low levels of compressible fluid sorption suggests that phase separation in multicomponent polymer/compressible solvent systems is not strictly analogous to that in polymer/liquid solvent systems.

Compressible solvents possess two important, distinguishing features relative to liquids: First, the quality of the solvent as quantified by density or dielectric constant can be systematically adjusted over broad

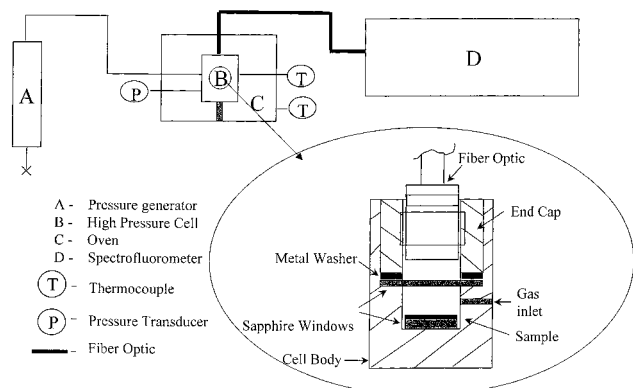
ranges by manipulating pressure, which provides a direct means to control the degree of solvent sorption. For example, Paulaitis reported that CO₂ sorption in polystyrene (PS) at 35 °C increases from 1.25 to 9.45 wt % as pressure is increased from 5 to 72 bar.¹⁰ If solvent sorption influences phase behavior predominantly through intersegment screening, as may be expected near the enthalpically driven upper critical solution temperature (UCST), controlling the degree of dilation with pressure should permit the location of the transition to be tuned directly. Recently, using SANS, we demonstrated that this is the case for nearly symmetric styrene-*block*-isoprene copolymers where the upper order–disorder transitions (UODT) are systematically depressed by increasing the severity of CO₂ or ethane sorption with pressure.⁹ A characterization that suggests that the sorption of compressible fluids is essentially equivalent to that of a homologous series of liquids with variable solvent strengths is, however, incomplete. While a low-density compressed fluid experiences a large reduction in volume upon sorption, the compressibility of the polymer/fluid mixture can increase substantially relative to that of the undiluted melt.¹¹ In multicomponent systems this factor, which is unique to compressible solvents, can lead to rapid and disparate increases in compressibilities of the mixture components that exacerbate the entropic penalty of mixing. Systems that exhibit LCST behavior, such as PS/PVME blends, should be particularly sensitive to this effect.

In this report, we present a detailed study of phase segregation in the PS/PVME/CO₂ system using in-situ high-pressure fluorescence spectroscopy. Next, the interaction between CO₂ and each of the homopolymers is examined, including determination of solvent quality by calculation of polymer–solvent interaction parameters from sorption data. We then present a semiquantitative comparison of the enthalpic and equation of state contributions to phase segregation in these systems based on stability arguments and the Sanchez–Lacombe equation of state (S–L EOS). Finally, we show that the S–L EOS can qualitatively predict phase separation of the blend upon sorption of CO₂.

* Corresponding author. E-mail: watkins@ecs.umass.edu.

Table 1. Characteristics of Polymers Used in This Study

component	M_n (kg/mol)	PDI	component	M_n (kg/mol)	PDI
PS-1	570	1.01	PS*	105	1.02
PS-2	83	1.02	PVME	90	3.0
PS-3	81	1.03	PVME	99	2.20

**Figure 1.** Equipment schematic for determination of high-pressure polymer phase behavior using fluorescence quenching.

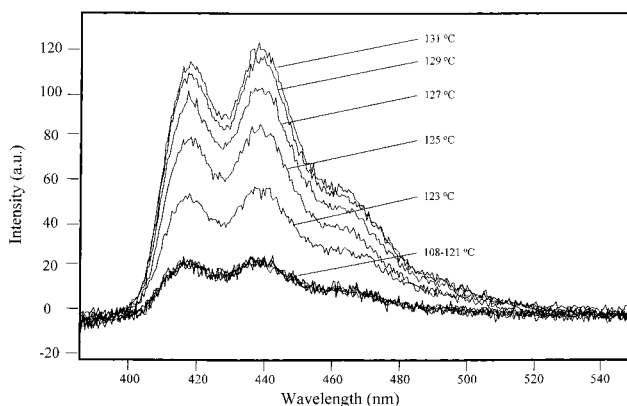
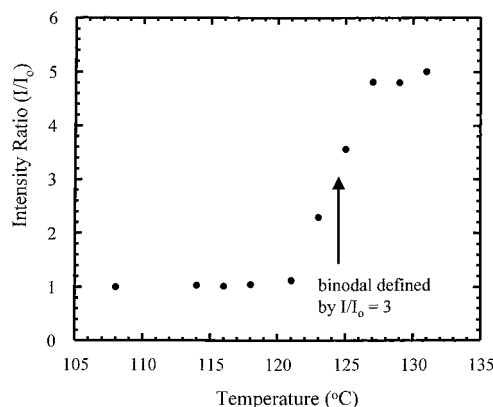
Experimental Section

Polystyrene (PS) and poly(vinyl methyl ether) (PVME) of different molecular weights were obtained from Polymer Source Inc. (Dorval, PQ Canada) and Scientific Polymer Products Inc. (Ontario, NY), respectively (Table 1). Prior to use, the PVME was dried in a vacuum oven at 60 °C for at least 24 h to remove water. Labeled polystyrene (PS*) containing a single anthracene tag at the center of each chain was obtained from Polymer Source Inc. and used as received. Carbon dioxide (Coleman Grade) was obtained from Merriam Graves. Prior to use, CO₂ was passed through oxygen and water traps.

Homogeneous PS/PVME and PS/PS*/PVME blends were prepared from toluene solutions (~7 wt % polymer). The mixtures containing PS* were doped such that concentration of the anthracene label in the solvent-free blend was approximately 10 ppm. Films (30–50 μm thick) were solvent-cast onto sapphire windows at room temperature and dried for at least 6 h in air and then at 60 °C for at least 10 h in a vacuum oven to ensure complete removal of residual toluene and moisture. The prepared films were stored under vacuum and transferred to a high-pressure cell immediately before use. Fluorescence spectra of anthracene (excitation 365 nm, emission monitored between 380 and 550 nm) were collected in front-face mode using a custom designed high-pressure cell (Figure 1) and a SPEX Fluoromax-2 spectrofluorometer equipped with a fiber-optic bundle. The cell was placed inside a custom-built convection oven. Temperature stability for isothermal experiments was ±1 °C. For experiments involving temperature profiles, the cell was fitted with a steel-heating jacket equipped with resistance cartridge heaters and a PID controller. All data were corrected using reference spectra collected for identical films undoped with PS* at identical pressure and temperature conditions. The reported fluorescence intensities are those taken at 415 nm using intensity at 540 nm as the baseline.

Results

Detection of discontinuities in the normalized emission intensity ratio of tagged PS as a function of temperature is a convenient and accurate method for the detection of phase separation in PS/PVME blends.¹² In the homogeneous state, PS* and PVME chains are intimately mixed, and anthracene fluorescence is quenched by the pendant ether oxygen of PVME. Upon

**Figure 2.** Anthracene fluorescence emission spectra of a 40/60 PS(83K)-PS*(105K)/PVME(99K) blend as a function of temperature at ambient pressure.**Figure 3.** Fluorescence intensity ratio (at 415 nm) for a 40/60 PS(83K)-PS*(105K)/PVME(99K) blend as a function of temperature. The LCST is 125 °C (see text).

phase separation, the anthracene tag is segregated from the quenching agent, as evidenced by a discontinuous increase in anthracene emission intensity. Figure 2 shows the anthracene emission spectra for a 40/60 PS/PVME blend as a function of temperature at ambient pressure. Initially, the system is phase-mixed as evidenced by the weak fluorescence signal. As temperature is increased through the coexistence temperature, anthracene emission increases rapidly, indicating the onset of phase separation. Figure 3 shows the emission intensity at 415 nm as a function of temperature for the experiment. We define phase separation as the point at which the fluorescence intensity ratio exceeds 3 times that of the homogeneous blend. The rates of heating for all ambient pressure experiments are small (1 °C/30 min). Data points obtained in this manner lie near the binodal (coexistence) curve.

This fluorescence quenching method can be readily adapted to study solvent-induced transitions at high pressure. Figure 4 shows the anthracene emission spectra for a 40/60 PS/PVME blend in the presence of compressed CO₂ as a function of pressure at 40 °C; above a pressure of approximately 16 bar the signal increases dramatically. In Figure 5, the emission intensity ratio at 415 nm as a function of pressure is shown for the experiment. We retain the criterion for phase separation ($I/I_0 \geq 3$) and define a phase separation pressure at 17 bar. Using these methods, we have generated phase diagrams for the blends using ambient pressure temperature profiles and isothermal pressure (density) profiles.

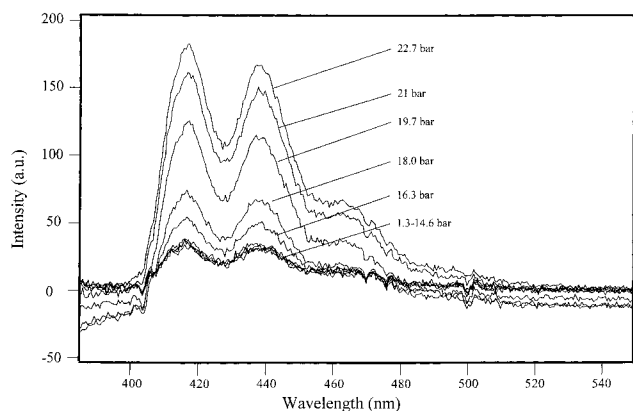


Figure 4. Anthracene fluorescence emission spectra of a 40/60 PS(83K)–PS*(105K)/PVME(99K) blend as a function of CO₂ pressure at 40 °C.

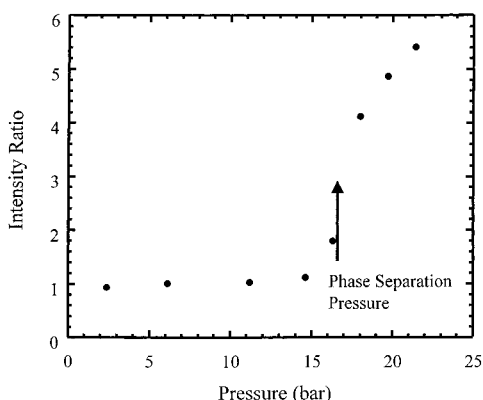


Figure 5. Fluorescence intensity ratio (415 nm) in a 40/60 PS(83K)–PS*(105K)/PVME(99K) blend as a function of CO₂ pressure at 40 °C. The phase separation pressure is 17 bar (see text).

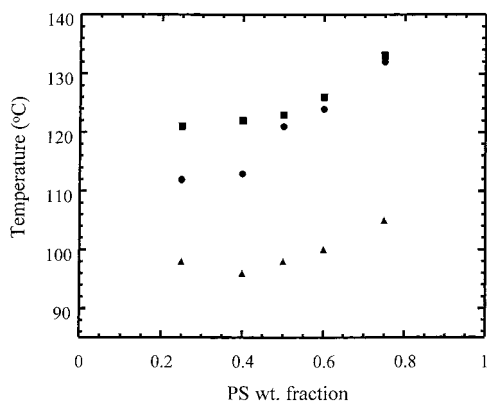


Figure 6. Phase diagram of PS/PVME blends as measured by fluorescence quenching: ■, 83K PS/99K PVME; ●, 570K PS/99K PVME; ▲, 81K PS/90K PVME. The polydispersity index is less than 1.05 for all PS samples, 2.2 for the 99K PVME, and 3.0 for the 90K PVME.

The location of the coexistence temperature for three PS/PVME binary blends as a function of PS concentration is shown in Figure 6. Note each of the PS samples is of narrow polydispersity, but the PVME samples exhibit PDIs of 2.2 and 3.0 for the 99 000 and 90 000 g/mol components, respectively. The thermally induced transitions measured in these experiments are in good agreement with literature data.¹³

The depression of the coexistence temperatures in the presence of CO₂ is shown in Figures 7 and 8. Each data point represents the onset of phase separation (defined

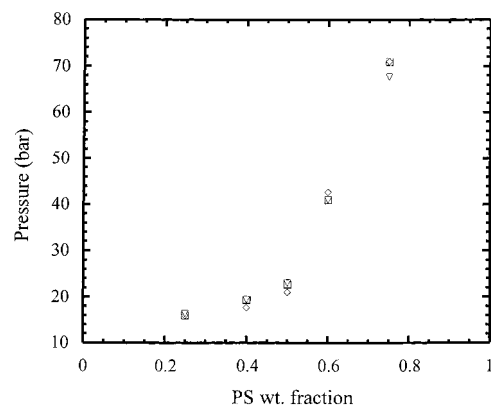


Figure 7. Phase separation pressure of PS/PVME blends in the presence of CO₂ at 40 °C as measured by fluorescence quenching: ◇, 83K PS/99K PVME; □, 570K PS/99K PVME; ▽, 81K PS/90K PVME.

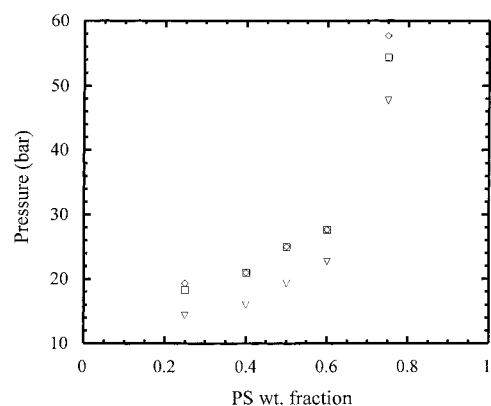


Figure 8. Phase separation pressure of PS/PVME blends in the presence of CO₂ at 60 °C as measured by fluorescence quenching: ◇, 83K PS/99K PVME; □, 570K PS/99K PVME; ▽, 81K PS/90K PVME.

Table 2. CO₂ Sorption Data in 50/50 Blends of PS/PVME at 20.6 °C and Calculated Sorption Isotherms and Solvent Densities at 40 and 60 °C

press (bar)	CO ₂ (wt fraction) in 50/50 PS/PVME at 20.6 °C ¹⁶	CO ₂ (wt fraction) in 50/50 PS/PVME at 40 °C	CO ₂ density at 40 °C (g/cm ³) ⁴⁵	CO ₂ density at 60 °C (g/cm ³) ⁴⁵
1.5	0.0031	0.00285	0.0025	0.0024
2.8	0.0064	0.00530	0.0048	0.0045
4.5	0.0103	0.00860	0.0078	0.0074
6.25	0.0174	0.0120	0.0110	0.0103
8.0	0.0226	0.01530	0.0142	0.0133
10.5	0.0286	0.0202	0.0189	0.0176
12.0	0.0320	0.0232	0.0217	0.0202
13.3	0.0352	0.0257	0.0242	0.0225
16.5	0.050	0.0320	0.0305	0.0282
18.0			0.0331	0.0305
20.0			0.0371	0.0342
22.0			0.0413	0.0379

by $I/I_0 \geq 3$) upon slow pressurization of the system with the compressible solvent. Solvent density at 40 and 60 °C is reported in Table 2, along with an estimate of total fluid sorption in the symmetric binary blend for each measurement in CO₂ at 40 °C as calculated using the Sanchez–Lacombe equation of state (see below).¹⁴ There are two remarkable features evident in the figures. First, the magnitude of the depression in the presence of CO₂ is striking, given the modest fluid densities and levels of CO₂ sorption. Second, the molecular weight dependence and the influence of polydispersity on the transition at 40 °C in the presence of CO₂ are lost. At

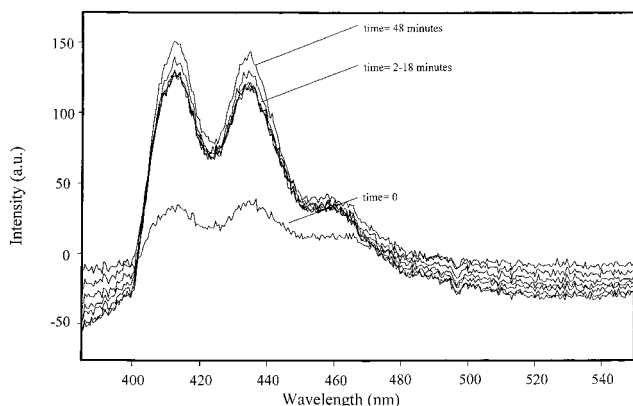


Figure 9. Increase of anthracene fluorescence emission as a function of time for a 75/25 PS(83K)–PS*(105K)/PVME(99K) blend during a pressure jump experiment in which the CO₂ vapor phase is compressed rapidly from ambient pressure to 79 bar at 40 °C. The results suggest PS/PVME phase separation is not subject to significant kinetic limitations at these conditions.

60 °C, these effects are highly attenuated; however, the CO₂-induced transition remains influenced by the PDI of PVME (Figure 8).

Most experiments were conducted well above the glass transition temperature (T_g) of the binary blends such that phase separation proceeds without significant kinetic limitations. This is clearly evident for the blends containing less than 50% PS, which have T_g 's less than 0 °C.¹⁵ Moreover, sorption of CO₂ can significantly depress the T_g of the polymeric components, which enhances mobility in the system. For example, the T_g of an 70/30 PS/PVME binary blend is approximately 32 °C, but sorption of CO₂ at approximately 10 bar is sufficient to induce a glass–rubber transition at 20.6 °C.^{15,16} Therefore, we cannot ascribe the collapse of the coexistence curves for the various blends to a common transition at 40 °C to proximity to the glass transition temperature. This conclusion is supported by rapid phase separation during an isothermal pressure jump experiment between the homogeneous and phase-separated regions of the PS/PVME/CO₂ phase diagram. Figure 9 shows a rapid increase in fluorescence intensity upon pressurization of CO₂ in contact with a 75/25 PS/PVME blend from ambient pressure to 79 bar at 40 °C. Phase separation at these conditions occurs within 2 min.

Discussion

In this section we consider potential mechanisms for phase separation in PS/PVME/CO₂ systems. First, the nature of LCST behavior in PS/PVME binary system is discussed. We then characterize the interactions between CO₂ and the homopolymers in the respective binary systems. Subsequently, we compare CO₂'s solvent strength and selectivity to that of traditional liquid solvents known to induce immiscibility in PS/PVME/solvent mixtures through the so-called “ $|\Delta\chi|$ ” effect. Next, we consider the relative importance of equation-of-state effects on polymer compatibility using a semi-quantitative stability analysis for a pseudobinary system comprised of PS/CO₂ and PVME/CO₂ as components based on the Sanchez–Lacombe equation of state. Finally, a stability analysis for the ternary system is shown to predict phase separation.

A. Binary PS/PVME Blends. For symmetric binary blends the well-known stability limit is $\chi N = 2$, where N is the number of chain segments.¹⁷ The requisite increase in χ necessary to induce the transition can be attributed to either enthalpic or entropic factors, acting alone or in combination.^{18,19} In systems with specific attractive segment–segment interactions such as hydrogen bonding and charge-transfer complex formation, the favorable enthalpic contribution to phase miscibility weakens with heating until it can no longer overcome the entropic penalty associated with maintaining contact-mediated preferred orientations of the interacting chain segments. In nonpolar systems that lack specific interactions, phase separation is attributed to negative volume changes upon mixing that arise due to the widening disparities between the free volumes of the phases as temperature is increased.

Phase segregation in PS/PVME blends has been studied using a variety of techniques including turbidimetry, differential scanning calorimetry, SANS, optical and electron microscopy, and fluorescence quenching.^{20–23} There is ample evidence that suggests both enthalpic and free volume considerations are important for PS/PVME binary systems. PS/PVME blends exhibit a charge-transfer interaction (π -hydrogen bond) between the electron-deficient methoxy proton in PVME and π -orbital in the aromatic ring of PS.²⁴ Riedl and Prud'Homme are among those that argue that a weakening of this interaction with increasing temperature is responsible for phase separation.²⁵ They used inverse gas chromatography to measure the interaction parameters between PVME and probes including benzene, which is a model for styrene. The interaction parameter was then partitioned into enthalpic and entropic contributions using a Flory–Patterson corresponding states approach with characteristic parameters that are corrected for thermal drift. They find that the benzene–PVME interactions decrease with increasing temperature, but the free volume contribution remains nearly constant. Other studies, however, find that the location of the LCST in PS/PVME is dependent on hydrostatic pressure, which suggests that free volume contributions are important. Hammouda and Janssen conducted independent SANS studies and found positive pressure coefficients for the LCST, $\Delta T_{LCST}/\Delta P$, ranging between 0.12 and 0.25 °C/MPa for PS/PVME blends depending on composition.^{26,27} Hammouda found that the entropic contributions to the SANS effective Flory interaction parameter, χ_{eff} , decreases with pressure (promoting miscibility) while the enthalpic contribution increased with pressure. Janssen reported a pressure dependence of the entropic contribution only, but subsequent reanalysis of the data yielded qualitative agreement with the results of Hammouda.²⁷ Dudowicz and Freed have shown that, within the framework of the lattice cluster theory, compressibility is necessary to explain the available PVT data for χ_{eff} , the heat and volume of mixing the components, and the location of the LCST. They conclude that the presence of excess free volume interferes with blend compatibility.²⁸ Finally, using numerical calculations based on the S–L EOS, Kumar and co-workers demonstrated that inclusion of compressibility is necessary to explain the composition dependence of the χ parameter and thus small-angle neutron scattering profiles from d-PS/PVME mixtures.²⁹

B. CO₂ Sorption in PS and PVME. To assess the effect of CO₂ sorption on blend phase behavior, it is useful to determine CO₂/polymer Flory–Huggins interaction parameters (χ 's). While CO₂ is a poor solvent for most polymers, it is soluble in and will dilate virtually all polymers, including PS and PVME. The CO₂ sorption data of Paulaitis for PS at 35 °C and the sorption data of Monnerie for PVME at 20.6 °C are shown in Figure 10a,b.^{10,16} The solid lines are our fits to the data using the Sanchez–Lacombe equation of state and the interaction parameters indicated in the legend (see section D). The sorption data can be used to calculate χ parameters using Flory's equation for the activity of a solvent in a polymer given by^{30–32}

$$\ln A_{\text{CO}_2} = \ln(1 - \phi_{\text{poly}}) + \left(1 - \frac{r_{\text{CO}_2}}{r_{\text{poly}}}\right)\phi_{\text{poly}} + \chi\phi_{\text{poly}}^2 \quad (1)$$

where A is the activity of CO₂, r is a size parameter, and ϕ_i is the volume fraction of component i . Here, we assume the ratio of the chain lengths (r) is equal to zero, owing to high molecular weights of the polymer. The advantage of calculations based on activity is that it superimposes both temperature and pressure of the gas into a single independent variable. The gas-phase fugacity of pure CO₂ was calculated using the Peng–Robinson equation of state. Using this method, we find $\chi_{\text{PS}/\text{CO}_2} = 1.6$ and $\chi_{\text{PVME}/\text{CO}_2} = 0.9$, indicating that CO₂ is a relatively poor solvent for both blend components but is selective for PVME.

C. Solvent Effects on Polymer Compatibility within an Incompressible Framework. Dilution of PS/PVME blends with highly selective good solvents can induce phase segregation for enthalpic reasons. The situation was described for spinodals and binodals by Patterson³³ and Prausnitz,³ respectively, using the incompressible Flory model for polymer(2)/polymer(3)/solvent(1) systems in which each of the binaries is miscible but the polymer–solvent interactions are asymmetric. The calculations indicate that at high polymer concentrations compatibility is governed by the interaction between the polymer segments ($\chi_{2,3}$), but at low concentrations, compatibility (or incompatibility) is dictated by differences between the polymer–solvent interaction parameters ($\chi_{1,2}$ and $\chi_{1,3}$). In the latter case, phase separation can occur when there is a large disparity in the strength of the polymer–solvent interactions. Patterson referred to this phenomenon as the “ $|\Delta\chi|$ ” effect ($|\Delta\chi| = |\chi_{1,2} - \chi_{1,3}|$).³⁴

Experimental verification of the “ $|\Delta\chi|$ ” effect can be found in PS/PVME/solvent systems at high dilution. PS and PVME form homogeneous blends due to a favorable π -hydrogen bond between the electron-deficient methoxy proton and the aromatic ring in styrene. Consequently, at low temperatures, the segment interaction parameter, $\chi_{\text{PS,PVME}}$, is slightly negative (~ -0.003 at 40 °C).³⁵ Thies found that homogeneous PS/PVME blends could be cast from cosolutions in tetrachloroethylene, benzene, toluene, and xylene, but the polymers are incompatible in chloroform, methylene chloride, or trichloroethylene.²¹ Su and Patterson measured interaction parameters for PS and PVME with a broad range of solvents, including those mentioned above (Table 3).³⁵ Consistent with the predictions of the Flory model, $|\Delta\chi|$ is small for the compatible solutions but large for solvents that induce incompatibility. The interaction parameters for each of the solvents that causes phase separation and

Table 3. Flory–Huggins Interaction Parameters for Various Solvents with PS and PVME at 25 °C³⁵

solvent	χ_{PS}	χ_{PVME}	solvent	χ_{PS}	χ_{PVME}
toluene	0.19	0.14	tetrachloroethene	0.36	0.34
chloroform	0.13	-0.92	benzene	0.26	0.15
trichloroethylene	0.19	-0.26	carbon dioxide ^a	1.6	0.9
dichloromethane	0.34	-0.39	cyclohexane	0.64	1.16

^a Parameters determined using eq 1.

PVME are large and negative. Thus, upon phase separation, the weakly attractive PS–PVME contacts are replaced with the energetically favored PVME–solvent contacts. Porter confirmed the relative strengths of these interactions in model chloroform solutions using ¹³C NMR.²⁴

The $|\Delta\chi|$ criteria can break down for systems in which the solvent is poor for both components. For example, homogeneous PS/PVME blends can be cast from cyclohexane despite a $|\Delta\chi|$ of 0.5 at 40 °C, which is larger than that of trichloroethylene.³⁵ Although the solvent is selective for PS over PVME, the interaction of cyclohexane with either polymer is much less favorable than the PS/PVME interaction.

We now consider the addition of CO₂ to a blend of PS and PVME in this context. While CO₂ is selective for PVME, it is a poor solvent for both components: neither polymer is soluble in CO₂, and solvent sorption in the blend is modest. Here $\chi_{\text{PS,CO}_2}$ and $\chi_{\text{PVME,CO}_2} \gg \chi_{\text{PVME,PS}}$. Phase segregation of PS and PVME would eliminate the most energetically favorable contacts in the system, and thus $\Delta\chi_{\text{interchange}}$ is positive. Under conditions of low diluent sorption, polymer compatibility in the ternary system should be governed by the preservation of the favorable polymer–polymer interactions. Nonetheless, sorption of less than 3.5% CO₂ in PS/PVME blends induces phase segregation. Moreover, the effects of molecular weight and polydispersity, which should be preserved in shifts of the phase boundaries induced by solvent screening of polymer contacts, are either lost or severely attenuated. Consequently, it is unlikely that segregation in the PS/PVME/CO₂ system is purely enthalpic in nature.

D. Compressibility and the LCST of PS/PVME/CO₂. We now examine the role of free volume (equation-of-state effects) as the potential driver for phase segregation in the PS/PVME and PS/PVME/CO₂ systems. The relative contributions of enthalpic and entropic factors to phase segregation can be drawn out by a stability analysis via differentiation of Gibbs free energy.³⁶ For a binary mixture, the stability criterion can be decomposed into compressible and incompressible contributions such that

$$g'' = g_{xx} - v\beta g_{vx}^2 > 0 \quad (2)$$

where g , β , and v are the Gibbs free energy, isothermal compressibility, and the specific volume of the system, respectively, and x is a composition variable such as mole or weight fraction. The first term on the right-hand side of the equation contains the constant volume interchange energy. The second term on the right contains the equation-of-state (free volume) contributions. Later, using a pseudobinary approach, we evaluate semiquantitatively each of these contributions to instability in the PS/PVME/CO₂ system. Equation 2 can be formally extended to ternary mixtures via

$$(g_{xx}g_{yy} - g_{xy}^2) - v\beta(g_{xx}g_{vx}^2 + g_{yy}g_{vy}^2 - 2g_{xy}g_{vx}g_{vy}) > 0 \quad (3)$$

where x and y are independent composition variables.

In eq 2, it is evident that any increase in compressibility tends to destabilize the system, irrespective of the other terms in the inequality. As a first step in the analysis, it is informative to determine the effect of compressed fluid sorption on the compressibility of multicomponent polymer melts. While these quantities are difficult to obtain experimentally, they are easily calculated using a suitable equation of state. The Sanchez-Lacombe equation of state¹⁴ is

$$\tilde{\rho}^2 + \tilde{P} + \tilde{T} \left\{ \ln(1 - \tilde{\rho}) + \left(1 - \frac{1}{r}\right) \tilde{\rho} \right\} = 0 \quad (4)$$

where \tilde{P} , \tilde{T} , and $\tilde{\rho}$ are the reduced pressure, temperature, and density, respectively, and r is a size parameter that represents the number of lattice sites occupied by a molecule. The reduced parameters are defined in terms of their characteristic parameters as

$$\tilde{T} = T/T^* \quad T^* = \epsilon^*/R \quad (5)$$

$$\tilde{P} = P/P^* \quad P^* = \epsilon^*/v^* \quad (6)$$

$$\tilde{\rho} = \rho/\rho^* \quad \rho^* = M/rv^* \quad (7)$$

where ϵ^* is the interaction energy per mer, R is the universal gas constant, v^* is the close-packed volume of a mer, and M is molecular weight. For a pure component the size parameter, r , is given by

$$r = \frac{P^* V^*}{RT^*} \quad V^* = Nv^* \quad (8)$$

where V^* is the close-packed volume of the N r -mers. Three characteristic parameters, available from regression of PVT data, are sufficient to completely characterize a pure component. The equation can be formally extended to mixtures using one temperature-dependent adjustable interaction parameter, δ_{ij} , in either P^* or ϵ^* . In this study, we use pairwise additivity of the characteristic pressure:

$$P^* = \sum_i \sum_j \phi_i \phi_j P_{ij}^* \quad (9)$$

the cross term is defined as

$$P_{ij}^* = \{P_i^* P_j^*\}^{1/2} (1 - \delta_{ij}) \quad (10)$$

The close-packed volume fraction of component i , ϕ_i , for binary mixtures is given by

$$\phi_i = \frac{m_i/\rho_i^*}{m_i/\rho_i^* + m_j/\rho_j^*} \quad (11)$$

where m_i is the weight fraction.

The mixing rule for v^* (the average close-packed mer volume) is

$$v^* = \phi_i^0 v_i^* + \phi_j^0 v_j^* \quad (12)$$

where the concentrations are given by

$$\phi_i^0 = \frac{m_i/\rho_i^* v_i^*}{\sum m_i/\rho_i^* v_i^*} \quad (13)$$

The mixing rule for T^* is¹⁴

$$\frac{T^*}{T} = \frac{\phi_i \tilde{T}_i + v \phi_j \tilde{T}_j}{\phi_i + v \phi_j} - \phi_i \phi_j \frac{\{P_i^* + P_j^* - 2P_{ij}^*\} v^*}{RT} \quad (14)$$

where

$$v = \frac{v_i^*}{v_j^*} \quad (15)$$

The value of δ_{ij} for PS/CO₂ and PVME/CO₂ is obtained by fitting the sorption data of Paulaitis (at 35 °C) and Monnerie (at 20.6 °C).^{10,16} The solubility of the polymer in the fluid phase is negligible. Thus, CO₂ sorption in homopolymers is modeled by equating the fugacities of pure CO₂ in the fluid phase (μ_1^0) and CO₂ sorbed in the polymer (μ_1^p) via³⁷

$$\frac{\mu_1^p}{kT} = \left\{ \ln \phi_1 + \left(1 - \frac{r_1}{r_2}\right) + r_1^0 \tilde{\rho} X_1 \phi_2^2 \right\} + r_1^0 \left\{ -\frac{\tilde{\rho}}{\tilde{T}_1} + \frac{\tilde{P}_1 \tilde{v}_1}{\tilde{T}_1} + \tilde{v} \left[(1 - \tilde{\rho}) \ln(1 - \tilde{\rho}) + \frac{\tilde{\rho}}{r_1^0} \ln \tilde{\rho} \right] \right\}$$

and

$$\frac{\mu_1^0}{kT} = r_1^0 \left\{ \frac{\tilde{P}_1 \tilde{v}_1}{\tilde{T}_1} - \frac{\tilde{\rho}_1}{\tilde{T}_1} + \tilde{v}_1 \left[(1 - \tilde{\rho}_1) \ln(1 - \tilde{\rho}_1) + \frac{\tilde{\rho}_1}{r_1^0} \ln \tilde{\rho}_1 \right] \right\} \quad (16)$$

where

$$X_1 = \frac{\{P_1^* + P_2^* - 2(P_1^* P_2^*)^{1/2} (1 - \delta_{ij})\} v_1^*}{RT}$$

Characteristic parameters for CO₂, PS, and PVME are taken from the literature (Table 4). Our fits of the data yield a binary interaction parameter of -0.042 for PVME/CO₂ and 0.045 for PS/CO₂. Sorption data are not available at 40 °C. Thus, while these interaction parameters are somewhat temperature dependent, we assume they are constant for our calculations over the limited temperature interval of 20–40 °C. We note that PS is initially a glass at the conditions of Paulaitis' sorption experiments (35 °C). Extension of the SL-EOS and other lattice fluid models to the glassy state formally requires the introduction of order parameters.³⁸ The PS/CO₂ sorption data of Paulaitis at 35 °C, however, span pressures at which PS is both above and below the depressed glass transition temperature. We fit only the data in the liquid regime to obtain a PS/CO₂ interaction parameter of 0.045 . We find,⁹ as did Johnston,³⁹ that in this case the sorption data at all pressures are well represented using only the binary interaction parameter.

The monomeric interaction parameter (δ_{ij}) between PS and PVME is determined using the Sanchez-Balasz (S-B) modification to the SL-EOS to fit experimental LCST curves obtained at ambient pressure.^{40,41} One advantage of the S-B modification is the incorporation

Table 4. Characteristic Parameters of Pure Components Used for Calculations with the Sanchez–Lacombe Equation

component	P^* (atm)	T^* (K)	ρ^* (g/cm ³)
polystyrene ³⁸	3530	735	1.105
poly (vinyl methyl ether) ³⁸	3580	657	1.100
carbon dioxide ³⁷	5670	305	1.510
chloroform ⁴⁶	4500	512	1.688
PS/PVME blend ^{38,39} (50/50)	3572	697	1.103

of a temperature dependence for the PS–PVME interaction through the mer–mer interaction energy of the mixture, ϵ^* . δ_{ij} is then obtained via calculation of the characteristic pressure of the mixture at the desired temperature using S–B theory and recovery of interaction parameter in the Sanchez–Lacombe formalism using eq 10. At 40 °C, $\delta_{PS-PVME}$ is found to be -0.00932 . We initially model sorption in the PS/PVME/CO₂ system using a pseudobinary mixture of a polymer (PS–PVME blend as a single component) and CO₂, wherein the polymer characteristic parameters are obtained from the blend LCST fit as above (Figure 10c).⁴⁰ Later, results of calculations using a ternary model and three binary interaction parameters are discussed.

The determination of the interaction parameter for the polymer/CO₂ mixture leads directly to the determination of specific volumes of the mixture at any inclusive or higher-pressure condition. At a given condition, we calculate the volume of the mixture as a function of hydrostatic pressure at constant composition. Compliant with its definition, compressibility is then obtained through the numerical differentiation via

$$\beta = \frac{-1}{v} \left[\frac{dv}{dP} \right]_{T,w} \quad (17)$$

Here, w is the mixture composition.

Figure 11 indicates that for the PS/PVME/CO₂ and PVME/CO₂ systems the compressibility of the mixture increases with increasing CO₂ pressure at 40 °C. This occurs for two reasons: First, CO₂ sorption in the mixture increases with pressure. Second, CO₂ is a high free volume diluent that increases compressibility of the mixture relative to that of the pure polymer. This is evident in the lattice-fluid context by examining T^* of the components and the resulting mixture, which provides a crude measure of free volume in the system. The mixing rule for T^* is given by eq 14. Sorption of CO₂ ($T^* = 305$ K) into PVME ($T^* = 657$ K), for example, substantially reduces T^* of the binary. Note this decrease can be quite large relative to the sorption of a liquid solvent such as chloroform ($T^* = 512$ K). This is evident in Figure 12, which shows the compressibility of CO₂/PVME and chloroform/PVME binaries at 20 and 25 °C, respectively, as a function of solvent weight fraction calculated using eq 17 over the range of available sorption data. The characteristic parameters for chloroform are listed in Table 4. The interaction parameter for the chloroform/PVME system was determined by fitting the vapor sorption data of Panayiotou and Vera.⁴² Also shown in Figure 11 is the compressibility of a PS/PVME blend under the influence of hydrostatic pressure only. The reduction in compressibility with hydrostatic pressure is consistent with the experimentally observed positive shift of the LCST at elevated pressure.^{26,27}

Fluid sorption dramatically increases both the system compressibility and magnifies the disparity between the

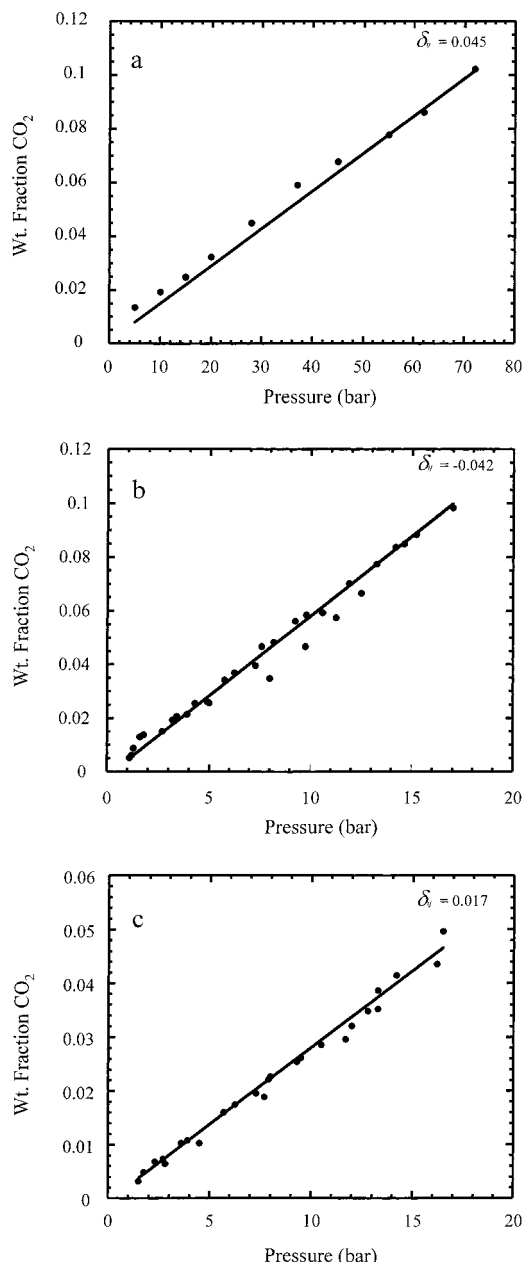


Figure 10. Fit of CO₂ sorption isotherms using the Sanchez–Lacombe EOS with characteristic parameters listed in Table 4 and the interaction parameter given in the insets: (a) polystyrene at 35 °C,¹⁰ (b) poly(vinyl methyl ether) at 20.6 °C,¹⁶ (c) 50/50 PS/PVME blend at 20.6 °C¹⁶ using a pseudobinary model.

compressibilities of the PVME/CO₂ and PS/CO₂ binaries. A qualitative measure of the free volume differences for two components in a polymer system can be obtained by examining the ratio of their characteristic temperatures⁴³ using

$$\tau = 1 - \frac{T_1^*}{T_2^*} \quad (18)$$

For polymer/polymer systems, τ is typically small (~ 0.15 or less); for polymer/solvent systems, τ is on the order of 0.4. The free volume mismatch in the latter case is largely responsible for the prevalence of LCST behavior in polymer solutions. A straightforward calculation of these T^* values for PS/CO₂ and PVME/CO₂ as two independent systems indicates that at a constant tem-

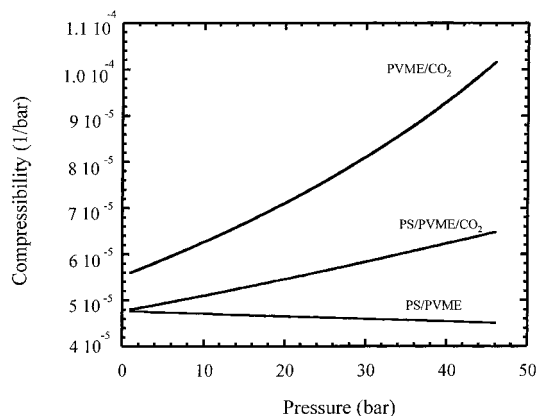


Figure 11. Compressibilities of different mixtures at 40 °C calculated using the Sanchez–Lacombe EOS.

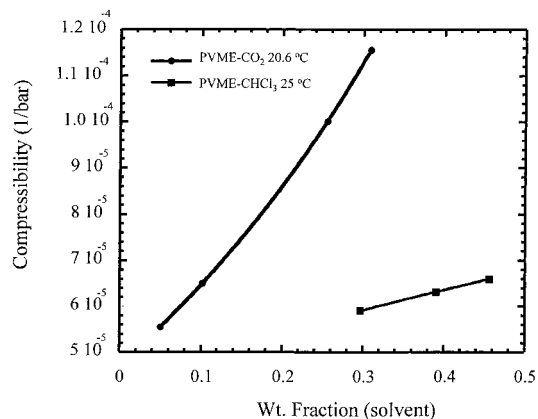


Figure 12. Compressibility of PVME/solvent binaries as a function of CO₂¹⁶ (●) and CHCl₃⁴² (■) weight fraction calculated using the Sanchez–Lacombe EOS over the range of available sorption data.

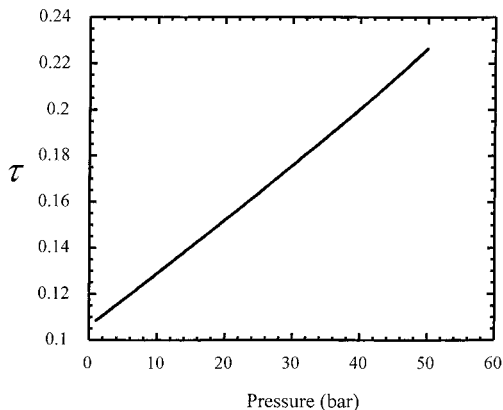


Figure 13. Increase in the free volume disparity between PS/CO₂ and PVME/CO₂ binaries as represented by the parameter τ ($\tau = 1 - T_1^*/T_2^*$) as a function of pressure at 40 °C calculated using CO₂ sorption data and the Sanchez–Lacombe equation of state.

perature of 40 °C they diverge with increasing pressure (Figure 13). The characteristic temperatures for CO₂, PVME, and PS are 305, 657, and 735 K, respectively. This divergence of the binary T^* s is a direct consequence of selective sorption of the high free volume diluent in the component with an inherently greater free volume. This will destabilize the pseudobinary mixture. Note also that, upon dilation of PS/PVME blends with CO₂, τ increases toward values that are characteristic of liquid solvent/polymer binary systems.

We now compare the free volume contribution to instability in the PS/PVME/CO₂ system relative to the enthalpic contribution using stability criterion for the LCSTs and the Sanchez–Lacombe EOS. Our objective is not to develop a predictive model for phase behavior in this system, but rather to identify the driving force for phase separation by applying lattice-fluid constructs to evaluate trends in these contributions to mixture instability. The calculations are performed isothermally using fixed values of the polymer/CO₂ and polymer/polymer interaction parameters. Quantitative predictions of the location of the phase transitions in blends using the SL-EOS are quite sensitive to the value of the interaction parameters for the mixture components, their temperature dependence, and thermal drift in the pure component parameters. Under isothermal conditions, concerns regarding potential artifacts arising from these temperature dependencies in the model are eliminated.

Consider mixing PS/CO₂ and PVME/CO₂ binaries to form the ternary system. It is now possible to evaluate eq 2 for the pseudobinary mixture using the Sanchez–Lacombe EOS. (We relax this assumption and evaluate the ternary directly later.) The chemical potential of component 1 in the mixture is given by the left-hand side of eq 16. Differentiation of eq 16 with respect to volume fraction at constant temperature and pressure yields the stability criterion.¹⁴

$$\frac{d(\mu_1/kT)}{d\phi_1} = 2r_1\phi_2 \left\{ \frac{1}{2} \left[\frac{1}{r_1\phi_1} + \frac{1}{r_1\phi_2} \right] - \tilde{\rho} \left[X + \frac{1}{2} \psi^2 \tilde{T} P^* \beta \right] \right\} \quad (19)$$

where ψ is a dimensionless parameter defined by

$$\psi = \frac{\tilde{\rho} \left[v \left(\frac{1}{\tilde{T}_1} - \frac{1}{\tilde{T}_2} \right) + (\phi_1^2 - v\phi_2^2) X_1 \right] - v \left(\frac{1}{r_1^0} - \frac{1}{r_2^0} \right) + \frac{\tilde{P}v(v-1)(\phi_1 + v\phi_2)}{\tilde{T}}}{(\phi_1 + v\phi_2)^2} \quad (20)$$

and

$$X = \frac{\{P_1^* + P_2^* - 2(P_1^*P_2^*)^{1/2}(1 - \delta_{ij})\} v^*}{RT} \quad (21)$$

The isothermal compressibility of the mixture is given by eq 16.

The system is stable if

$$\frac{1}{2} \left[\frac{1}{r_1\phi_1} + \frac{1}{r_1\phi_2} \right] - \tilde{\rho} \left[X + \frac{1}{2} \psi^2 \tilde{T} P^* \beta \right] > 0 \quad (22)$$

The form of eq 22 reveals the motivation for the pseudobinary approach. The term on the far left is the combinatorial entropy term, $\tilde{\rho}X$ is an energetic contribution, and $1/2\tilde{\rho}\psi^2\tilde{T}P^*\beta$ is the entropic contribution from the equation-of-state effects. These contributions to miscibility for the pseudobinary system PS/CO₂ + PVME/CO₂ as a function of pressure at constant temperature can be evaluated using the EOS by calculating the characteristic parameters of the components (PS/CO₂ and PVME/CO₂) at the conditions of interest using sorption data. The combinatorial term for the pseudobinary must be positive and thus will stabilize the mixture. We note, however, that its magnitude will be overestimated since CO₂ sorption in the blend is slightly

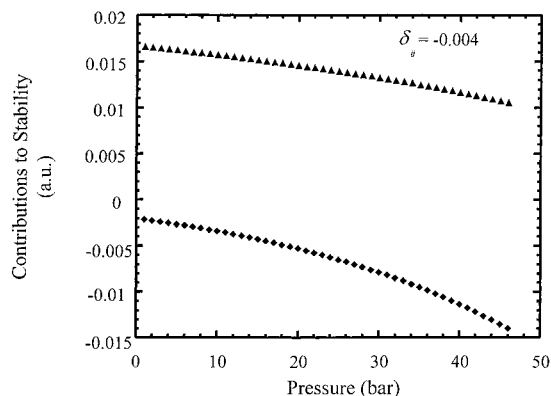


Figure 14. Contributions to the enthalpic ($-\tilde{\rho}\chi$) (\blacktriangle) and noncombinatorial entropy ($-1/2\tilde{\rho}\psi^2\tilde{T}P^*\beta$) (\blacklozenge) terms to the stability of the pseudobinary mixture of PS/CO₂ and PVME/CO₂ at 40 °C using the Sanchez–Lacombe equation of state.

less than the weighted average of sorption in the individual polymers.⁴⁴ Figure 14 shows the result of the calculation for the energetic and equation-of-state contributions by fixing δ_{ij} for the pseudobinary at -0.004 for all CO₂ pressures. Upon fluid sorption, the contribution of the $1/2\tilde{\rho}\psi^2\tilde{T}P^*\beta$ term clearly destabilizes the system. It is driven primarily by the increasing disparity of the characteristic temperatures of the pseudobinary components as the degree of CO₂ sorption increases with pressure (see Figure 13). The interchange energy (enthalpic) contribution to stability decreases slightly due to dilution of the favorable PS–PVME contacts upon increasing CO₂ sorption with pressure but remains favorable. These calculations were repeated using values of δ_{ij} ranging between that of PS/PVME (-0.00932), the most attractive interactions in the system, and 0.0. Adjusting δ_{ij} within these limits does not alter the conclusions of the analysis. The enthalpic contribution remains positive within this range but increases in magnitude, as δ_{ij} becomes more negative. Its slope is determined by the characteristic parameters of the pseudobinary components, which are (CO₂) pressure (and therefore composition) dependent, but is insensitive to the value of the pseudobinary interaction parameter. The favorable combinatorial and unfavorable noncombinatorial entropic contributions to the free energy are largely insensitive to the value of δ_{ij} . Thus, while a fully predictive model for phase behavior requires precise knowledge of δ_{ij} at the conditions of interest, it is not required to identify the primary driving force for phase separation in this case.⁴⁷

The pseudobinary approximation for the PS/PVME/CO₂ system can be relaxed, and the stability criterion for the ternary mixture can be evaluated directly by differentiation of the Gibbs free energy as prescribed by

$$\begin{vmatrix} g_{xx} & g_{xy} & g_{x\tilde{v}} \\ g_{yx} & g_{yy} & g_{y\tilde{v}} \\ g_{\tilde{v}x} & g_{\tilde{v}y} & g_{\tilde{v}\tilde{v}} \end{vmatrix} > 0 \quad (23)$$

where x and y are two independent composition variables and \tilde{v} is the reduced volume of the system.³⁶ Since each of the three binary interaction parameters is known independently, the calculation can in principle be conducted without any additional parameters. It is instructive to first assess how the EOS formalism performs for predicting the solubility of CO₂ in the

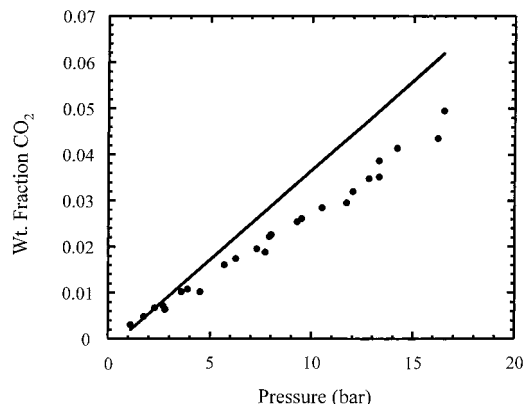


Figure 15. CO₂ sorption data (\bullet) in a 50/50 PS/PVME blend¹⁶ and a sorption isotherm calculated directly for the ternary system using the Sanchez–Lacombe EOS at 20.6 °C and the three independent binary interaction parameters.

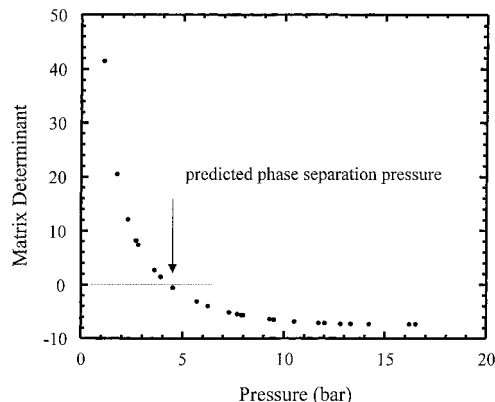


Figure 16. Stability analysis for the ternary system PS/PVME/CO₂ at 40 °C using the Sanchez–Lacombe EOS. The determinant becomes negative, indicating phase separation at pressures above 5 bar.

ternary system. Figure 15 indicates the results of the calculation are qualitatively correct but do not provide precise agreement with experimental data. The prediction of the stability of the ternary system using the Sanchez–Lacombe EOS is given in Figure 16. The EOS accurately predicts a phase split upon CO₂ sorption as indicated by a sign change in the determinant, but the prediction of phase separation pressure of CO₂ is in slight error. Lack of precise quantitative agreement is not surprising given the well-known sensitivity of these calculations to the values of the interaction parameters. Such agreement could be obtained via the use of an additional mixture parameter for the ternary system, but such an exercise does not lend additional insight into the nature of the transition.

Conclusions

Sorption of carbon dioxide, a compressible, selective, poor solvent, causes a dramatic reduction in the coexistence temperature of PS/PVME blends. The magnitude of the depression (>90 °C) upon sorption of modest amounts of the diluent (~ 3.5 wt %) is incommensurate with solvent screening of polymer/polymer contacts and clearly overwhelms the effect of hydrostatic pressure, which promotes miscibility in these systems. A stability analysis using the Sanchez–Lacombe lattice-fluid equation of state is used as a vehicle to compare the relative importance of enthalpic and equation-of-state contributions to phase instability in these systems. The results

indicate the phase behavior is dominated by a disparity in the free volume (dilation) of the polymer components upon sorption of CO₂, which exacerbates the entropic penalty of mixing.

In the PS/PVME/CO₂ system, the polymer component of higher intrinsic compressibility (PVME) is preferentially dilated with the high free volume diluent (CO₂), which may account for the severity of the depression. We have observed similar effects in the block copolymer polystyrene-*block*-poly(*n*-butyl methacrylate) in the presence of CO₂ where selective dilation of the polyacrylate block leads to depressions of the lower disorder—order transition by over 200 °C: we expect this to be a general result for systems exhibiting LCST behavior. Future work will focus on the effects of fluid sorption for gases that exhibit selectivity for the polymer component of lower intrinsic compressibility. We are also examining the effect of CO₂ sorption in blends such as polyisoprene/polybutadiene that do not exhibit an attractive interaction between the polymer components and which exhibit low selectivity for CO₂.

Acknowledgment. This work was supported by the NSF Materials Research Science and Engineering Center at the University of Massachusetts and the David and Lucile Packard Foundation.

References and Notes

- Scott, R. L. *J. Chem. Phys.* **1949**, *17*, 279.
- Tompa, H. *Trans. Faraday Soc.* **1949**, *45*, 1140.
- Hsu, C. C.; Prausnitz, J. M. *Macromolecules* **1974**, *7*, 320.
- Patterson, D. *Polym. Eng. Sci.* **1982**, *22*, 64.
- Fredrickson, G. H.; Leibler, L. *Macromolecules* **1989**, *22*, 1238.
- Hong, K. M.; Noolandi, J. *Macromolecules* **1983**, *16*, 1083.
- Lodge, T. P.; Pan, C.; Jin, X.; Liu, Z.; Zhao, J.; Maurer, W. W.; Bates, F. S. *J. Polym. Sci., Phys. Ed.* **1995**, *33*, 2289.
- Watkins, J. J.; Brown, G. D.; RamachandraRao, V. S.; Pollard, M. A.; Russell, T. P. *Macromolecules* **1999**, *32*, 7737.
- Vogt, B. D.; Brown, G. D.; RamachandraRao, V. S.; Watkins, J. J. *Macromolecules* **1999**, *32*, 7907.
- Wissinger, R. G.; Paulaitis, M. E. *J. Polym. Sci., Phys. Ed.* **1987**, *25*, 2497.
- Garg, A.; Gulari, E.; Manke, C. W. *Macromolecules* **1994**, *27*, 5643.
- Halary, J. L.; Ubrich, J. M.; Nunzi, J. M.; Monnerie, L.; Stein, R. S. *Polymer* **1984**, *25*, 956.
- Ubrich, J. M.; Larbi, F. B. C.; Halary, J. L.; Monnerie, L.; Bauer, B. J.; Han, C. C. *Macromolecules* **1986**, *19*, 810.
- Sanchez, I. C.; Lacombe, R. H. *Macromolecules* **1978**, *11*, 1145.
- Tsujita, Y.; Kato, M.; Kinoshita, T.; Takizawa, A. *Polymer* **1992**, *33*, 773.
- Mokdad, A.; Dubault, A.; Monnerie, L. *J. Polym. Sci., Phys. Ed.* **1996**, *34*, 2723.
- De Gennes, P.-G. *Scaling Concepts in Polymer Physics*; Cornell University Press: Ithaca, NY, 1979.
- Siow, K. S.; Delmas, G.; Patterson, D. *Macromolecules* **1972**, *5*, 29.
- Sanchez, I. C.; Panayiotou, C. In *Models for Thermodynamic and Phase Equilibria Calculations*; Sandler, S. I., Ed.; Marcel Dekker Inc.: New York, 1994; p 187.
- Yang, H.; Hadziioannou, G.; Stein, R. S. *J. Polym. Sci., Phys. Ed.* **1983**, *21*, 159.
- Bank, M.; Leffingwell; Thies, C. *J. Polym. Sci.* **1972**, *A-2*, 1097.
- Davis, D. D.; Kwei, T. K. *J. Polym. Sci., Phys. Ed.* **1980**, *18*, 2337.
- Nishi, T.; Wang, T. T.; Kwei, T. K. *Macromolecules* **1975**, *8*, 227.
- Djordjevic, M. B.; Porter, R. S. *Polym. Eng. Sci.* **1982**, *22*, 1109.
- Riedl, B.; Prud'homme, R. E. *J. Polym. Sci., Phys. Ed.* **1990**, *28*, 2411.
- Hammouda, B.; Bauer, B. J. *Macromolecules* **1995**, *28*, 4505.
- Janssen, S.; Schwahn, D.; Mortensen, K.; Springer, T. *Macromolecules* **1993**, *26*, 5587.
- Dudowicz, J.; Freed, K. F. *Macromolecules* **1995**, *28*, 6625.
- Kumar, S. K.; Veytsman, B. A.; Maranas, J. F.; Crist, B. *Phys. Rev. Lett.* **1997**, *79*, 2265.
- Flory, P. J. *Principles of Polymer Chemistry*; Cornell University: Ithaca, NY, 1953.
- Berens, A. R.; Huvard, G. S. In *Supercritical Fluid Science and Technology*; Johnston, K. P., Penninger, J. M. L., Eds.; American Chemical Society: Washington, DC, 1989; p 207.
- Edwards, R. R.; Tao, Y.; Xu, S.; Wells, P. S.; Yun, K. S.; Parcher, J. F. *J. Phys. Chem. B* **1998**, *102*, 1287.
- Zeman, L.; Patterson, D. *Macromolecules* **1972**, *5*, 513.
- Robard, A.; Patterson, D.; Delmas, G. *Macromolecules* **1977**, *10*, 706.
- Su, C. S.; Patterson, D. *Macromolecules* **1977**, *10*, 708.
- Sanchez, I. C. In *Polymer Compatibility and Incompatibility Principles and Practices*; Solc, K., Ed.; MMI Press Symposium Series Vol. 2; Harwood Academic Publishers: Chur, Switzerland, 1982; p 59.
- Kiszka, M. B.; Meilchen, M. A.; McHugh, M. A. *J. Appl. Polym. Sci.* **1988**, *36*, 583.
- Wissinger, R. G.; Paulaitis, M. E. *Ind. Eng. Chem. Res.* **1991**, *30*, 842.
- Condo, P. D.; Sanchez, I. C.; Panayiotou, C. G.; Johnston, K. P. *Macromolecules* **1992**, *25*, 6119.
- Sanchez, I. C.; Balazs, A. C. *Macromolecules* **1989**, *22*, 2325.
- An, L.; Wolf, B. A. *J. Macromol. Sci., Pure Appl. Chem.* **1997**, *A34* (9), 1629.
- Panayiotou, C.; Vera, J. H. *Polym. J.* **1984**, *16*, 89.
- Patterson, D.; Robard, A. *Macromolecules* **1978**, *11*, 690.
- Hachisuka, H.; Takanori, S.; Tsujita, Y.; Takizawa, A.; Kinoshita, T. *Polym. J.* **1989**, *21*, 417.
- Lemmon, E. W.; McLinden, M. O.; Friend, D. G. *Thermophysical Properties of Fluid Systems*. In *NIST Chemistry WebBook*; NIST Standard Reference Database No. 69; Mallard, W. G., Linstrom, P. J., Eds.; National Institute of Standards and Technology: Gaithersburg, MD, Nov 1998 (<http://www.webbook.nist.gov>).
- Sanchez, I. C.; Lacombe, R. H. *J. Phys. Chem.* **1976**, *80*, 2352.
- In our analysis it is assumed δ_{ij} is negative for the pseudo-binary. This is a valid assumption at low levels of CO₂ solution and must be true as the pressure approaches ambient (and CO₂ solubility approaches zero). We point out, however, that use of a positive δ_{ij} renders the energetic contribution negative, but its slope, which is determined by the characteristic parameters of the mixture components, is considerably more shallow than that of the free volume term. Thus, the free volume contribution is the dominant contributor to instability for any value of δ_{ij} .

MA000066E